Desalination and Water Treatment
www.deswater.com
doi: 10.1080/19443994.2013.827298

52 (2014) 784–790
January

Taylor & Francis
Taylor & Francis Group

Modelling of phosphorus removal by ion-exchange resin (Purolite FerrIX A33E) in fixed-bed column experiments

T. Nur[a], W.G. Shim[b], M.A.H. Johir[a], S. Vigneswaran[a,*], J. Kandasamy[a]

[a]*Faculty of Engineering and Information Technology, University of Technology, Broadway, Sydney NSW 2007, Australia*
Email: s.vigneswaran@uts.edu.au
[b]*School of Applied Chemical Engineering, Chonnam National University, Gwangju 500-757, Korea*

Received 23 March 2013; Accepted 5 May 2013

ABSTRACT

Phosphorus removal is important as it causes eutrophication that in turn has a harmful effect on fish and other aquatic life, resulting in a reduction in biodiversity as well as unfavourable human environmental health. In this study, phosphorus removal from aqueous solutions was studied using an ion-exchange resin (Purolite FerrIX A33E) in fixed-bed column experiments. The effects of adsorbent bed height (3–19 cm) on the breakthrough characteristics of the adsorption system were studied. An increase in bed height (3–19 cm) increased adsorption capacity but the breakthrough time was shorter. As the bed height increased, the detention time increased and the phosphate was in contact with the purolite ion-exchange resin for a longer time, resulting in more efficient removal of phosphate. The shape of breakthrough curve was steeper for a shorter bed height. A mathematical model (advection—dispersion equation) was solved numerically to predict the dynamic behaviour of the columns. Finally, sensitivity analysis results apparently revealed that the dynamic adsorption behaviours of phosphate in Purolite FerrIX A33E were mainly controlled by the external mass transfer rather than the axial dispersion and the intra-particle diffusion.

Keywords: Eutrophication; Ion-exchange resin; Fixed-bed column; Breakthrough curve; Advection—dispersion equation

1. Introduction

Phosphorus is an essential nutrient for growth of both vegetable plants and micro-organisms and also a very important material for many industries. But the extensive industrial use of phosphorus produces excess phosphate-bearing waste that can disturb the balance of organisms present in water. The excess phosphorus reaches water environment as diluted waste that can affect the water quality through the depletion of the dissolved oxygen level as the algae decay. There is a harmful effect on fish and other aquatic life because of this depletion of the oxygen level in water bodies, which in turn causes

---

*Corresponding author.

Presented at the Fifth Annual International Conference on "Challenges in Environmental Science & Engineering—CESE 2012" Melbourne, Australia, 9–13 September 2012

eutrophication. Eutrophication is one of the most environmental problems, as it can lead to abundant development of aquatic plants, growth of algae and disturb the balance of organisms present in the water. Phosphorus removal is important to control eutrophication and to maintain a sustainable green environment for the forthcoming generation.

On the other hand, the recovery of phosphorus is very important to minimize the future global phosphorus scarcity that is likely to be one of the greatest challenges of the twenty-first century. Phosphorus rock, the main source of phosphorus at present, is non-renewable and becoming increasingly scarce and expensive and peak phosphorus was estimated to occur by 2035, after which demand would outstrip supply [1]. Phosphorus is very essential for food production as it is a key ingredient in fertilizers to sustain high crop fields for all life (e.g. plants, animals and bacteria). For this reason, it is very important to develop a recovery process for phosphorus from phosphorus containing wastewater as an alternative source of phosphates to compensate for such global exhaustion of high-grade phosphate ores.

Several physical, biological and chemical processes have been investigated for the removal of dissolved phosphorus in water and wastewaters. Among the various methods of phosphorus removal, adsorption/ion exchange method is promising, because it allows simple and economical operation, resulting in less sludge production, and therefore, minimal disposal problems. Furthermore, this method seems to be the most suitable for small water supplies contaminated by phosphorus because of its simplicity, effectiveness, selectivity, recovery and relatively low cost [2]. This method also has the ability to handle shock loadings and the ability to operate over a wide range of temperatures. A variety of adsorbents have also been developed for selectively remove phosphate, such as aluminium oxide, iron oxide, zirconium oxide, ion-exchange resin such as purolite, hydrotalcite [3] and layered double hydroxides [4].

Fixed-bed sorption processes are ideal for the reduction of dissolved phosphate to near-zero level provided the sorbent is phosphate selective, cost-effective and amenable to efficient regeneration and reuse for several cycles of operation. Commercial anion exchangers, granular-activated alumina, iron oxides, zirconium oxides and hydrotalcite are a well-studied adsorbents in this regard. Their performances with regard to phosphate removal with varying degrees of success are well documented in the literature [5]. Majority of the studies reported in literature on adsorptive removal of phosphate from water were conducted in batch type of adsorption experiments. The results from these studies cannot be directly applied to real system of water treatment, where fluid flows continuously through a column of adsorbent or a packed bed involving dynamic adsorption of the solute. The columnar operation allows more efficient utilization of the adsorptive capacity than the batch process. The adsorbent at the inlet end is contacted continuously by the solution at the initial solute concentration and the change in concentration at each subsequent layer is small. Therefore, the adsorbent in the column acts like a series of layers, with each layer in contact with a fresh solution of constant solute concentration. This procedure results in maximum loading of the adsorbent at constant solute concentration, and is in contrast to the continuously declining solute concentration in batch process.

The aim of this present research is to study and model the removal of phosphorus from synthetic wastewater through the use of an ion-exchange resin called Purolite FerrIX A33E in fixed-bed systems. The effects of bed height were investigated in this study and then a numerical model was developed to solve the advection—dispersion equation with adsorption in columns.

2. Materials and methods

2.1. Ion-exchange resins

The commercially available and economically reasonable strong-base anion exchange resin, Purolite FerrIX A33E was used as an adsorbent in this study. The physical and chemical characteristics of Purolite FerrIX A33E are presented in Table 1. Purolite FerrIX A33E media is a nanoparticle derived selective resin designed to remove arsenic (arsenate & arsenite) from the water supply [6]. Purolite FerrIX A33E unites a unique blend based on hydrous iron oxide nano

Table 1
Typical chemical and physical characteristics of Purolite FerrIX A33E [6]

Parameters	Purolite FerrIX A33E
Polymer matrix structure	Polystyrene cross-linked with divinylbenzene
Physical form and appearance	Brown spherical beads
Particle size	0.3–1.2 mm
Relative density	1.15–1.30
Moisture retention, Cl^- form	35–65%
Operating temperature, Cl^- form	40°C

particles that have a very high attraction for arsenic with a durable, non-friable, spherical polymer substrate.

2.2. Feed solution

The feed solution was prepared using KH_2PO_4 with distilled water spiked with different concentrations of phosphate (5–30 mg P/L).

2.3. Chemical analysis

The analysis of phosphate ion was carried out using Metrohm ion chromatograph (model 790 Personal IC) equipped with an auto sampler and conductivity cell detector. The separation was achieved using an A SUPP column 3 (150 mm × 4 mm). Na_2CO_3 (3.2 mmol/L) and $NaHCO_3$ (1.0 mmol/L) were used as mobile phase with the actual flow rate of 0.7 mL/min.

2.4. Column mode experiments

The fixed-bed column was made of Pyrex glass tube of 2.5 cm inner diameter (Fig. 1). At the bottom of the column, a stainless steel sieve was attached followed by a layer of glass beads in order to provide a uniform flow of the solution through the column. A known quantity (12–86 g) of the purolite was packed in the column to yield the desired bed height (3–19 cm) of the adsorbent. Phosphate solution of known concentrations (20 mg P/L) was pumped upward through the column at a desired filtration velocity (2.5 m/h) controlled by a peristaltic pump. The effluent at the outlet of the column was collected at regular time intervals and the phosphate concentration was measured using ion chromatograph.

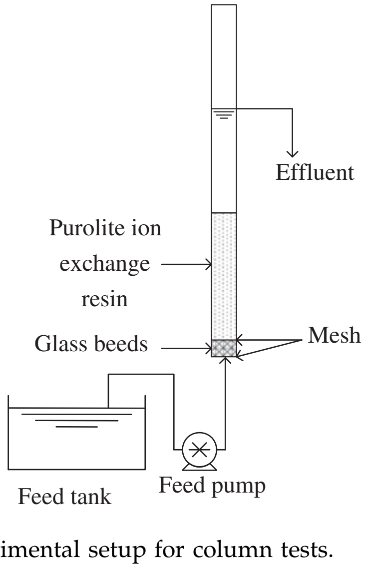

Fig. 1. Experimental setup for column tests.

2.5. Fixed-bed numerical modelling

In order to formulate the dynamic model of fixed-bed adsorber charged with ion-exchange resin, the following assumptions are used: (1) The system is under isothermal conditions; (2) The flow pattern is an axially dispersed plug flow and the radial concentration gradient is insignificant; (3) The shape of ion-exchange resin is spherical, and its pore structure is uniform; (4) The liquid film mass transfer resistance at the outer surface of the solid particles can be described by a driving force; (5) Intra-particle diffusion can be characterized by the homogeneous surface diffusion model (HSDM); (6) Adsorption equilibrium isotherm can be represented by the Langmuir equation.

The mass balance equations and the boundary conditions of the fixed-bed system are given by the following equations, which were previously derived by [7–9].

$$\frac{\partial C}{\partial t} = D_L \frac{\partial^2 C}{\partial z^2} - V\frac{\partial C}{\partial z} - \frac{1-\varepsilon_b}{\varepsilon_b}\frac{3k_f}{R}(C - C_s) \tag{1}$$

where C (mg/L) is the phosphate concentration in the adsorber at any given time and position, C_s (mg/L) is the phosphate concentration at the particle–liquid film interface, t (min) is the time, z (m) is the axial coordinate, D_L (m^2/s) is the axial dispersion coefficient, V (m/s) is the interstitial velocity, ε_b (−) is the bed void age, R (m) is the particle radius of adsorbent and k_f (m/s) is the film mass transfer coefficient, respectively.

The above equation can be solved by using the initial and boundary conditions, $C = 0$ and $z = 0$,

$$D_L \frac{\partial C}{\partial z}\bigg|_{z=0} = -v(C|_{z=0^-} - C|_{z=0^+}) \tag{2}$$

and at $z = L$,

$$\frac{\partial C}{\partial z}\bigg|_{z=L} = 0 \tag{3}$$

The mass transfer rate was also described by HSDM [10,11].

The homogeneous surface diffusion equation can be expressed as:

$$\frac{\partial q}{\partial t} = D_s\left(\frac{\partial^2 q}{\partial r^2} + \frac{2\partial q}{r\partial r}\right) \tag{4}$$

Initial and boundary conditions are:

$$t = 0;\ q = 0 \tag{5}$$

$$r = 0;\ \frac{\partial q}{\partial r} = 0 \tag{6}$$

$$r = r_{\mathrm{p}};\ D_{\mathrm{s}}\rho_{\mathrm{p}}\frac{\partial q}{\partial r} = k_{\mathrm{f}}(C - C_{\mathrm{s}}) \tag{7}$$

where q is surface concentration at any radial distance (r) from the centre of the particle during adsorption, mg N/g; D_{s}, the surface diffusion coefficient (the rate of diffusion of the nitrate along the surface of the adsorbent), m^2/s; k_{f}, the external mass transfer coefficient, m/s; ρ_{p}, the apparent density of the adsorbent, $\mathrm{kg/m}^3$; C, the bulk phase concentration, mg N/L; C_{s}, the concentration on the external surface, mg N/L.

The Langmuir isotherm (Eq. (8)) is used to describe the adsorption equilibrium relationship between liquid and solid phase concentrations.

$$q = \frac{q_{\mathrm{m}}\mathrm{b}C}{1 + \mathrm{b}C} \tag{8}$$

Axial dispersion coefficient, D_{L}, can be estimated from the following empirical correlation introduced by Delgado [12,13].

$$\frac{1}{\mathrm{Pe_L}} = \frac{\mathrm{Pe_m}}{5}(1 - p^2) + \frac{\mathrm{Pe_m^2}}{25}p(1 - p)^3 \times \left\{\exp\left[-\frac{5}{p(1 - p)\mathrm{Pe_m}}\right] - 1\right\} + \frac{1}{\tau\mathrm{Pe_m}} \tag{9}$$

$$p = \frac{0.48}{\mathrm{Sc}^{0.15}} + \left(\frac{1}{2} - \frac{0.48}{\mathrm{Sc}^{0.15}}\right)\exp\left(-\frac{75Sc}{\mathrm{Pe_m}}\right) \tag{10}$$

where $\mathrm{Pe_L}$, $\mathrm{Pe_m}$, Sc and τ are the Peclet number for axial dispersion, Peclet number for particle, Schimdt number and the tortuosity, respectively.

The external mass transfer coefficient, k_{f}, is estimated from the following empirical correlation equation depicted by Chu et al. [14]:

$$k_{\mathrm{f}} = 5.7V_{\mathrm{s}}\mathrm{Re}^{-0.75}\mathrm{Sc}^{-0.67} \tag{11}$$

where Re, Sc and V_{s}, are Reynolds number, Schimdt number and superficial velocity, respectively.

The molecular diffusion coefficient, D_{m}, can be calculated using the following the Wilke–Chang equation [15]:

$$D_{\mathrm{m}} = 7.4 \times 10^{-8}\frac{(\phi M_{\mathrm{b}})^{1/2}T}{\mu V_{\mathrm{a}}^{0.6}} \tag{12}$$

where ϕ, M_{b}, T, μ and V_{a} are an association factor of solvent, molecular weight of solvent, temperature, viscosity of solvent and solute molar volume at its normal boiling temperature, respectively.

In order to simulate the experimental breakthrough curves, one need to solve the dynamic equations described in above, which consist of bulk and solid phase concentration simultaneously. In this study, the orthogonal collocation method and the variable coefficient ordinary differential equation solver are used for that purpose [16–19].

3. Results and discussions

3.1. Fixed-bed column studies

Adsorption of phosphorus by Purolite Ferrix A33E was presented in the form of breakthrough curves. In these curves, the concentration ratio C_{t}/C_0 was plotted against time. Here, C_{t} and C_0 were the effluent and influent phosphate concentrations in mg/L, respectively. The breakthrough curves became less sharp, when the mass transfer rates were decreased [20]. Since mass transfer rates were finite, the breakthroughs were diffused and exhibited an S-shape.

Fig. 2 shows the breakthrough curves obtained for phosphate adsorption on the purolite resin at bed heights of 3, 6, 12, 14, 16, 17 and 19 cm (12, 28, 56, 66, 76, 80 and 86 g of resin), at a constant filtration

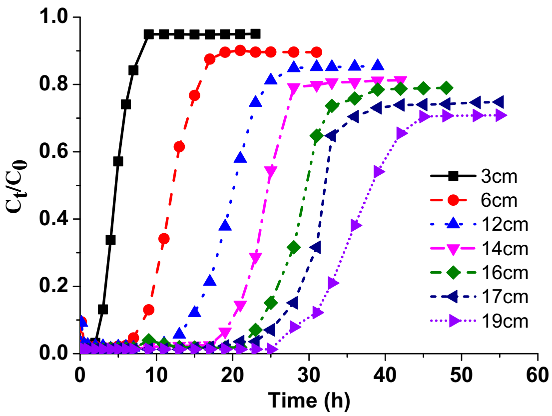

Fig. 2. Breakthrough curve for different bed heights (initial concentration = 20 mg/L as P and flow rate = 2.5 m/h).

velocity 2.5 m/h and inlet concentration of 20 mg P/L. From Fig. 2 and it is seen that, at low-bed heights, the breakthrough occurred faster than that at high-bed heights. This pattern of breakthrough at different bed heights was similar to the findings in other column studies on different adsorbents and adsorbates [11,21,22]. The starting time of saturation occurred after 3, 9, 13, 19, 23, 25 and 28 h, when the bed height was 3, 6, 12, 14, 16, 17 and 19 cm, respectively, and the 50% saturation was achieved within the interval of 5, 13, 21, 25, 31, 34 and 39 h, respectively. The columns were fully saturated (plateau zone of $C_t/C_{0)}$ in the interval of 9, 19, 27, 31, 40, 40 and 45 h for filter depths of 3, 6, 12, 14, 16, 17 and 19 cm, respectively. The corresponding values of C_t/C_0 were 0.95, 0.90, 0.85, 0.80, 0.78, 0.74 and 0.70. As the bed height increased, phosphate had more time to contact with the purolite ion-exchange resin that resulted in higher removal efficiency of phosphate. Thus, the higher bed height resulted in a decrease in phosphate concentration in the effluent. The slope of the breakthrough curve decreased with increase in bed height as a result of broadened influent movement zone [21,22]. However, it was found that the complete pattern of adsorption breakthrough curve was formed at all bed heights. The adsorption of phosphate increased with increase in the bed height from 3 to 19 cm, because of the increased amount of adsorption sites available at higher bed heights. This was reflected from the breakthrough with a bed height of 3 cm, where the adsorbent got saturated earlier as compared with at higher bed depths.

3.2. Fixed-bed numerical modelling

3.2.1. Effect of bed length

The effect of bed length (height) on adsorption breakthrough curves at inlet concentrations (22–24 mg/L) and the constant inlet filtration velocity (2.5 m/h) were shown in Fig. 3 with simulation results. The adsorption breakthrough curves appeared earlier and their shapes also became slightly sharper (or steeper), when the bed height was shorter. However, the shapes of the concentration curve were stable and completely formed, which indicates that the constant pattern behaviours were established for all testing conditions. Fixed-bed model predictions with different empirical coefficients gave reasonable fits to the experimental data although some deviations were observed. The values of kinetic parameters (D_L, k_f and D_S) for different bed heights were given in Table 2. The values of mass transfer coefficient (k_f) and the axial dispersion coefficient (D_L) for different bed heights were same and only a very little effect on the rate of intra-particle diffusion (D_s) that was similar to the results reported by Koh et al. [23].

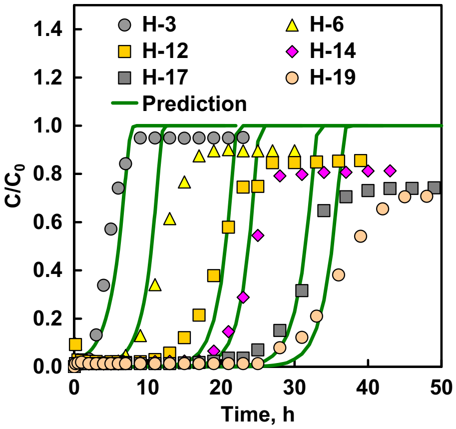

Fig. 3. Effect of bed length on the adsorption breakthrough curves.

3.2.2. Sensitive analysis

The sensitivity analysis has been carried out to examine the influence of the core parameters, D_L, k_f and D_s, on the adsorption behaviour. In this study, the reference breakthrough curve was taken from the fixed-bed results with an influent concentration of 34.8 mg/L, a bed length of 12 cm, and an influent

Table 2
Experimental conditions and kinetic parameters for phosphate adsorption on Purolite FerrIX A33E

Run no.	Length cm	Velocity l/min	Feed concentration ppm	$D_L^* \times 10^6\,m^2/s$	$k_f^{**} \times 10^6\,m/s$	$D_S^{***} \times 10^{10}\,m^2/s$
L-1	3	2.5	21.6	1.297	3.598	1.167
L-2	6		24.0			1.183
L-3	12		24.0			1.183
L-4	14		24.3			1.185
L-5	17		22.0			1.170
L-6	19		22.0			1.170

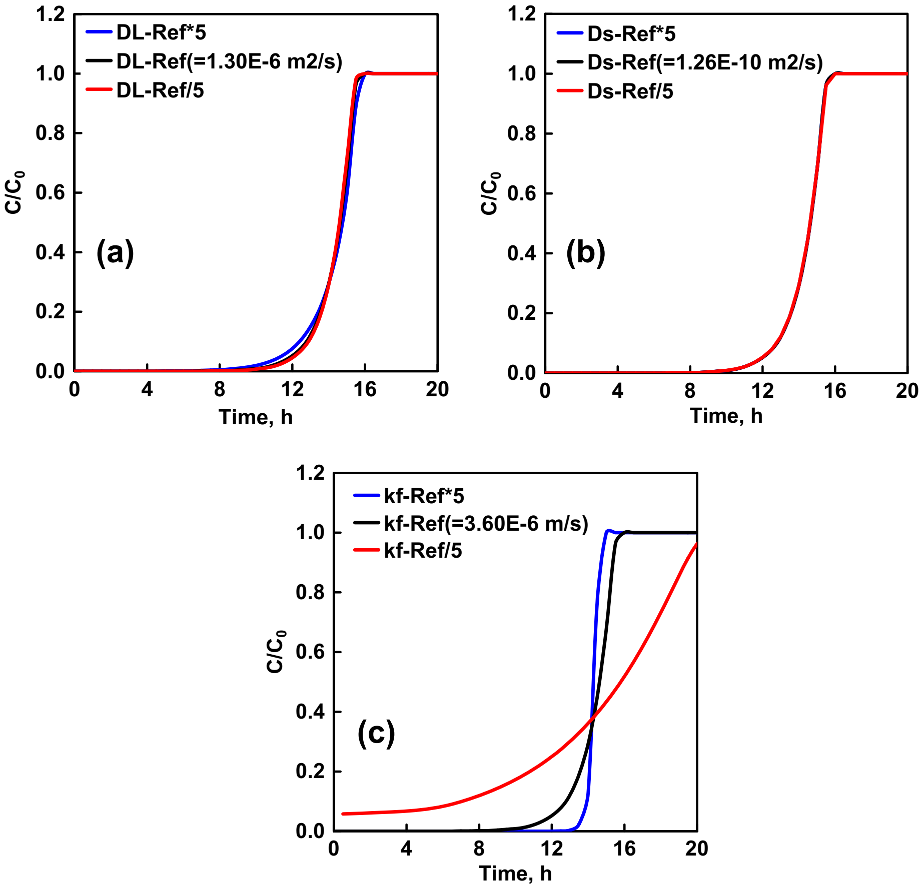

Fig. 4. Effect of model parameters on the adsorption breakthrough curve: (a) Axial dispersion, (b) External mass transfer, (c) Homogeneous surface diffusivity.

filtration velocity of 2.5 m/h, respectively. To systematically investigate the pattern of adsorption breakthrough curve, each parameter values were changed between 5 times lower and 5 times greater than that of the reference one. It was clear from Fig. 4 that the shapes of breakthrough curves for phosphate were highly sensitive to changes in the external mass transfer, k_f. However, the breakthrough curves were slightly sensitive or insensitive to variations in both the axial dispersion, D_L and the intra-particle diffusivity, D_S. These results apparently revealed that the dynamic adsorption behaviours of phosphate in Purolite FerrIX A33E were mainly controlled by the external mass transfer rather than the axial dispersion and the intra-particle diffusion.

4. Conclusion

The ion-exchange resin Purolite FerrIX A33E showed satisfactory results for removing phosphorus from aqueous solutions using fixed-bed adsorption column. The adsorption capacity was increased with the increasing of bed height. The advection—dispersion equation including the adsorption term (Eq. (1)) was considered as a mathematical model to simulate the ion-exchange process in columns packed with ion-exchange resins. Fixed-bed model predictions with different empirical coefficients gave reasonable fits to the experimental data although some deviations were observed at different adsorbent bed height, influent phosphorus concentration and filtration rate. According to sensitivity analysis, each parameter values were changed between 5 times lower and 5 times greater than that of the reference one for systematically investigation of the pattern of adsorption breakthrough curve. The dynamic adsorption behaviours of phosphate on Purolite FerrIX A33E were mainly controlled by the external mass transfer rather than the axial dispersion and the intra-particle diffusion.

Acknowledgement

This study was funded by Australian Research Council Discovery Research Grand (DP 1092603). Thanks Vitachem for supplying Purolites.

References

[1] D. Cordell, J.O. Drangert, S. White, The story of phosphorus: Global food security and food for thought, Sci. Technol. 19 (2009) 292–305.

[2] M. Boumediene, D. Achour, Denitrification of the underground waters by specific resin exchange of ion, Desalination 168 (2004) 187–194.

[3] P.A. Terry, Removal of nitrates and phosphates by ion exchange with hydrotalcite, Environ. Eng. Sci. 26 (2009) 691–696.

[4] L. Lv, P. Sun, Y. Wang, H. Du, T. Gu, Phosphate removal and recovery with calcined layer double hydroxides as an adsorbent, Phosphorus Sulfur 183 (2008) 519–526.

[5] F.X. Pollio, R. Kunin, Tertiary treatment of municipal sewage effluents, Environ. Sci. Technol. 2 (1968) 54–61.

[6] www.purolite.com-Purolite FerrIX A33E, Technical data, ISO 9002.

[7] C. Tien, Adsorption Calculations and Modeling, Butterworths-Heinemann, Boston, MA, 1994.

[8] D.M. Ruthven, Principles of Adsorption and Adsorption Processes, John Wiley, New York, 1984.

[9] R.T. Yang, Gas Separation by Adsorption Processes, Butterworths, Boston, MA, 1986.

[10] S. Vigneswaran, D.S. Chaudhary, H.H. Ngo, W.G. Shim, H. Moon, Application of. A PAC-membrane hybrid system for removal of organics from secondary sewage effluent: Experiments and modeling, Sep. Sci. Technol. 38 (2003) 2183–2199.

[11] R.T. Ahmad, T.V. Nguyen, W.G. Shim, S. Vigneswaran, H. Moon, J. Kandasamy, Effluent organic matter removal by purolite® A500PS: Experimental performance and mathematical model, Sep. Purif. Technol. 98 (2012) 46–54.

[12] J.M.P.Q. Delgado, Mass transfer and dispersion around an active cylinder in cross flow and buried in a packed bed, Heat Mass Transf. 42 (2006) 279–310.

[13] A. Jourak, I. Herrmann, V. Frishfelds, T.S. Lundström, A. Hedström, Modeling of phosphate removal by filtra P in fixed-bed columns, 2nd International Conference on Environmental Science and Technology (ICEST). (2011) 1119–1128.

[14] J.C. Chu, J. Kalil, W.A. Wetteroth, Mass transfer in a fluidized bed, Chem. Eng. Prog. 49 (1953) 141–149.

[15] C.R. Wilke, P. Chang, Correlation of diffusion coefficients in dilute solutions, AIChE J. 1 (1955) 264–270.

[16] J. Villadsen, M.L. Michelsen, Solution of Differential Equation Models by Polynomial Approximation, Prentice-Hall, Englewood Cliffs, NJ, 1978.

[17] P.N. Brown, G.D. Byrne, A.C. Hindmarsh, VODE: A variable coefficient ODE solver, SIAM J. Sci. Stat. Comput. 10 (1989) 1038–1051.

[18] J.M. Abdul, S. Vigneswaran, W.G. Shim, J. Kandasamy, Removal of metsulfuron methyl by granular activated carbon adsorption, Desalin. Water Treat. 21 (2010) 247–254.

[19] W.G. Shim, J.M. Abdul, T. Mohammad, S. Vigneswaran, H.H. Ngo, J. Kandasamy, Biofilter in leachate treatment processes, Desalin. Water Treat. 41 (2012) 249–257.

[20] J. N. Cloutier, A. Leduy, R. S. Ramalho, Peat adsorption of herbicide 2,4-D from wastewater, Can. J. Chem. Eng. 63 (1985) 250–257.

[21] M.M. Sekhula, J.O. Okonkwo, C.M. Zvinowanda, N.N. Agyei, A.J. Chaudhary, Fixed bed column adsorption of Cu (II) onto maize tassel-PVA beads, J. Chem. Eng. Process Technol. 3(2) (2012) 1–5, doi: 10.4172/2157-7048.1000131.

[22] N.K.E.M. Yahaya, I. Abustan, M.F.P.M. Latiff, O.S. Bello, M. A. Ahmad, Fixed–bed column study for Cu (II) removal from aqueous solutions using rice husk based activated carbon, J. Eng. Technol. 11 (2011) 248–252.

[23] J.-H. Koh, P.C. Wankat, N.-H.L. Wang, Pore and surface diffusion and bulk-phase mass transfer in packed and fluidized beds, Ind. Eng. Chem. Res. 37 (1998) 228–239.